Photoneutron spectroscopy using monoenergetic gamma rays for bulk explosives detection

J. E. McFee[a], A. A. Faust[a], K. A. Pastor[b]

[a] *Defence R&D Canada – Suffield, Medicine Hat, Canada*
[b] *McMaster University, Hamilton, Canada*

Abstract

To date, the most successful nuclear methods to confirm the presence of bulk explosives have been radiative thermal neutron capture (thermal neutron activation) and prompt radiative emission following inelastic fast neutron scattering (fast neutron analysis). This paper proposes an alternative: photoneutron spectroscopy using monoenergetic gamma rays. If monoenergetic gamma rays whose energies exceed the threshold for neutron production are incident on a given isotope, the emitted neutrons have a spectrum consisting of one or more discrete energies and the spectrum can be used as a fingerprint to identify the isotope. A prototype compact gamma-ray generator is proposed as a suitable source and a commercially available ^{3}He ionization chamber is proposed as a suitable spectrometer. Advantages of the method with respect to the previously mentioned ones may include simpler spectra and low inherent natural neutron background. Its drawbacks include a present lack of suitable commercially available photon sources, induced neutron backgrounds and low detection rates. This paper describes the method, including kinematics, sources, detectors and geometries. Simulations using a modified Geant4 Monte Carlo modelling code are described and results are presented to support feasibility. Further experiments are recommended.

Keywords:
Photoneutron spectroscopy, Monoenergetic gamma rays, Monte Carlo simulation, Neutron spectrometer, Bulk explosives detection, Compact gamma-ray source, Helium-3 ionization chamber
PACS: 25.40.Lw, 29.90.+r, 07.07.Df

1. Introduction

The detection and identification of hidden bulk explosives by neutron and gamma-ray interrogation has been investigated for over six decades [1, 2]. Of the four general classes of such reactions: neutrons in/neutrons out, neutrons in/photons out, photons in/photons out, photons in/neutrons out, the first three have been extensively studied. Examples which have shown some success are neutron backscatter, thermal neutron activation and fast neutron analysis, and X-ray backscatter imaging [3, 4, 5]. Although photoneutron reactions were the first to be studied for explosives detection [1], photon in/neutron out reactions have received little attention for this application.

Bulk nitrogen is a strong indicator of the presence of buried military explosives, such as RDX and TNT, since they possess nitrogen in large percentages but nitrogen is virtually absent in soil. However, in some detection scenarios such as baggage handling, a few benign items with high nitrogen content may be found. Additionally, bulk hydrogen and carbon can be indicators of both military and homemade explosives (HME). Hydrogen is ubiquitous in most scenarios and, unless imaged, is not a very useful indicator for explosives detection [6]. In buried explosives scenarios, the carbon in organic materials and certain carbonaceous soils might provide some false alarms, since carbon concentrations in soil range from 0.1 to over 9% by weight, depending on soil type [1].

In this paper, we propose a previously uninvestigated method of explosives detection: photoneutron spectroscopy with monoenergetic gamma rays. Assume that a beam of monoenergetic gamma rays in the energy range from 6-12 MeV were incident on an explosive target. If the incident gamma-ray energy exceeded the Q-value for neutron production in the target materials, and if the energy spread was small with respect to the level spacing of the residual nuclei, neutrons of discrete energies (neutron groups) would be emitted. Furthermore, if an energy-sensitive neutron detector with very good energy resolution (small with respect to the level spacing) were employed, the spectrum of emitted characteristic neutrons might be used to identify nuclei associated with explosives (H, C, N, O). For example, a monoenergetic 11.668-MeV photon beam incident on a sample of TNT would yield ~ 1.035-MeV neutrons from the ^{14}N$(\gamma, \mathrm{n})^{13}$N reaction and other monoenergetic neutron groups, corresponding to the various isotopes of H, C, N and O within the sample. The method requires both a monoenergetic gamma-ray source and a high resolution neutron spectrometer. We propose a compact accelera-

tor based on a low energy proton beam for the former and a special ^{3}He ionization chamber for the latter.

Photoneutron spectroscopy may have some advantages compared to thermal neutron capture for bulk explosives detection. First, for similar materials, photoneutron spectra may be simpler than neutron capture gamma-ray spectra because the reaction energetics limit the number of excited states available to be populated, compared to thermal neutron capture. The simplicity may make it possible to reduce the interference of competing background and target materials. Second, natural surroundings do not spontaneously emit fast neutrons, whereas background gamma rays are common. There are disadvantages, as well. At present there is no commercially available, compact source of gamma rays in the required energy range. This may change in the near future. Background rates from photoneutron emission in the shielding and background materials are unknown, but based on experience with linear accelerators, may be moderately high. Modelling and experimentation can answer this question and can suggest suitable shielding materials and configurations. Finally, the use of the technology for the particular application represents unknown territory and there may be as yet unanticipated problems. Since photoneutron spectroscopy with a monoenergetic gamma-ray source for bulk explosives detection has never been done, its promise is yet to be explored.

1.1. Background

Between 1947 and 1951, the Armour Research Foundation of the Illinois Institute of Technology studied detection of neutrons from simulated land mines in soil boxes, using a bremsstrahlung beam whose endpoint energy was slightly higher than the 10.553-MeV ^{14}N(γ, n)^{13}N Q-value. The neutron detectors lacked energy discrimination and so the approach failed due to a strong background of neutrons from silicon [1]. No further measurements of photoneutron reactions specifically for land mine detection have been reported since.

Photoneutron detection of ^{13}C and ^{2}H was also suggested but dismissed. If an incident photon energy of 6 MeV were to be used, only those two isotopes would be excited. However, without neutron energy discrimination, down-scattered fast neutrons from the deuterium in water would dominate the response [1]. A suggested alternative to detecting the prompt neutron emission is to detect the annihilation radiation from the positron decay of ^{13}N ($t_{1/2}$ = 9.96 m), but theoretical considerations have ruled it out due to low signals and high backgrounds [1]. The lack of further research in explosives detection using photoneutrons can be attributed to a lack of portable high resolution neutron spectrometers and a lack of a fieldable source of monoenergetic gamma rays in the appropriate energy range.

The most commonly used neutron detectors in the energy range of 100 keV to a few MeV, proton recoil scintillators and time-of-flight (TOF) spectrometers, are not suitable for practical detection of bulk explosives. A resolution of at least $\sim$ 30 keV at 1 MeV is required (see Section 2). Proton recoil scintillation neutron spectrometers typically achieve roughly 100-200 keV in the 1- to 2.5-MeV range [7, 8] for monoenergetic neutrons but the required spectral unfolding can make resolution much worse for complicated neutron spectra. They are also sensitive to gamma rays. To achieve sufficient energy resolution, TOF spectrometers become too large ($\sim$ 3.1 m flight path) and have too low an efficiency [9]. The high resolution ^{3}He Shalev-Cuttler type ionization chamber [10, 11], while much less commonly used, turns out to be a suitable neutron spectrometer for the present application.

There are presently a few ways to achieve a monoenergetic photon beam in the required energy range. These include the stepped bremsstrahlung method, tagged photon beams, positron annihilation in flight, thermal neutron capture on a nuclear reactor core target and a variety of charged particle reactions [12] using particle accelerators, such as a Van de Graaff. Only the latter two techniques have sufficiently small energy spreads and all of them involve large particle accelerators or reactors which are impractical for bulk explosive detection scenarios. They are discussed more fully in Ref. [9].

In the last few years, several research groups have been developing compact gamma-ray accelerator-based generators exploiting the ^{11}B(p, γ)^{12}C and ^{19}F(p, $\alpha\gamma$)^{16}O reactions to produce 11.668- and 6.128-MeV gamma rays. These sources are presently laboratory proof-of-concept prototypes but have the promise to become commercially available. Further, intense ^{241}Am/^{13}C isotopic sources could be used to produce 6.128-MeV gamma rays, with a weak neutron background. With both the necessary neutron spectrometer and gamma-ray sources now potentially available, the feasibility of the method should be examined in detail.

Photoneutron spectroscopy with monoenergetic gamma rays is a novel method for detection of bulk explosives. In a 1981 report [13], one of the authors suggested using a Shalev-Cuttler ionization chamber for explosives detection. Photoneutron spectra of heavy nuclei had previously been obtained using such a spectrometer and a beam of monoenergetic gamma rays from a nuclear reactor beam port [14, 15]. However, at that time, compact monoenergetic gamma-ray generators for energies in the 6- to 12-MeV range were not available. The present method, with the addition of the compact gamma-ray source, was first introduced in 2010 [9].

The present paper analyzes the method in greater depth, primarily through a modelling study. The relevant theory will be outlined, followed by descriptions of the detector and the compact source which are required for practical applications. A simple geometry, which is typical and practical for buried explosives detection, is described. The modelling study has been conducted to answer a number of questions, prior to start-

ing experiments. Questions include whether the neutron groups are sufficiently separated to allow material identification and whether elastic scattering of neutrons has a significant effect on energy broadening. Background photoneutron rates and expected count rates from targets in the typical geometry are estimated. Results from the modelling study are presented. Although the geometry is related to explosives buried in soil, many of the results can be generalized to other explosives detection applications. Finally, conclusions with suggested experiments and future plans are presented.

2. Theory

2.1. Kinematics

When a target nucleus having atomic number Z and atomic mass $A + 1$, undergoes a photoneutron reaction ${}^{A+1}_{Z}\mathrm{X}(\gamma,\mathrm{n}){}^{\mathrm{A}}_{Z}\mathrm{X}$, the kinetic energy of the emitted neutron E_n can be shown to be approximated by,

$$E_n = (E_\gamma - Q - E_x)/(1 + 1/A) \quad (1)$$

where E_γ is the gamma-ray energy, Q is the reaction Q-value and E_x is the excitation energy of the resultant nucleus [9]. For large A, Equation 1 is accurate to within a few keV for gamma rays in the 6-12-MeV range. Equation 1 shows that the corresponding neutron energies will form a set of discrete values independent of emission angle, provided the width of E_γ is much less than the energy separation and width of the excited states. (For the exact solution, see Ref. [9].)

Kinematic restrictions due to the finite longitudinal momentum of the incident photon impose constraints on the range of neutron emission angles. However, for the combinations of E_γ, $Q + E_x$ and A used this study, it can be shown that all neutron emission angles are possible [9].

Table 1 shows most of the discrete neutron energies that would be observable if a monoenergetic 11.668-MeV beam of gamma rays were used to irradiate a military explosive in soil[1]. Neutron energies are based on Equation 1, using nuclear excited state energies from Firestone *et al* [16]. The 1.035-MeV neutron from ${}^{14}\mathrm{N}(\gamma,\mathrm{n}){}^{13}\mathrm{N}$ and the 0.779-MeV neutron from ${}^{15}\mathrm{N}(\gamma,\mathrm{n}){}^{14}\mathrm{N}$ could be used to identify the presence of most explosives, including all military explosives. The 1.023-MeV neutron from ${}^{30}\mathrm{Si}$ is not resolvable from the 1.035-MeV nitrogen neutron (the resolution of the neutron spectrometer of Section 3.1 at 1-MeV neutron energy is <30 keV), but the percentage abundance of ${}^{30}\mathrm{Si}$ is small. Furthermore, the higher energy Si neutron intensities can be used, in principle, to correct for the intensity at 1.023 MeV.

[1]Typical abundances of elements in explosives and soil can be found in [1]. Elemental argon is found in air at a concentration of 0.93%.

Table 1 also shows the neutron energies for a monoenergetic 6.128-MeV gamma-ray beam. The spectrum is much simplified with only three neutron groups, one each from H, C, O. The presence of carbon is often a good indicator of explosives, since only a few soils have carbon concentrations high enough to provide significant false positive rates [1]. Combined with the oxygen signal, stoichiometric ratios could be used to identify the presence of many energetic materials, including non nitrogen-based explosives, such as triacetone triperoxide (TATP).

2.2. Energy Broadening

For light target nuclei, which are of interest in our problem, Equation 1 is only approximate and there is a small but significant dependence on neutron emission angle. For example, 11.668-MeV gamma rays incident on ${}^{30}\mathrm{Si}$ produce ground state neutrons with energies of 1.030 ± 0.010 MeV for $0° \leq \theta < 180°$. For a ${}^{14}\mathrm{N}$ target, the ground state neutron energies are 1.050 ± 0.020 MeV for the same angular range. The former spread is close to, and the latter exceeds, the nominal energy resolution of the neutron spectrometer at that energy. However, for practical backscatter geometries expected for bulk explosives detection, the angular range is more restrictive and the neutron energy spread is less. As an example, for the geometry of the present study (Section 4), the relevant neutron emission angle is in the range $130° \leq \theta < 180°$ and the neutrons have an energy spread of 1.036 ± 0.004 MeV for ${}^{30}\mathrm{Si}$ and 1.063 ± 0.007 MeV for ${}^{14}\mathrm{N}$. As can be seen, the angular dependence also serves to displace the centroid of the neutron energies. When angular dependence is ignored, the separation in energy between the ${}^{30}\mathrm{Si}$ and ${}^{14}\mathrm{N}$ ground state neutrons is 12 keV (Table 1), whereas in the backscatter geometry, the centroids are separated by 27 keV.

The spectrum of emitted photoneutrons can be further broadened by elastic scattering in the target or surrounding materials [9]. The energy broadening can be substantial, particularly for light scattering nuclei. For example, the ratio of scattered neutron energy to initial neutron energy varies from 0 to 1.0 for ${}^{1}\mathrm{H}$, 0.75 to 1.0 for ${}^{14}\mathrm{N}$ and 0.866 to 1.0 for ${}^{28}\mathrm{Si}$. The fraction of the neutrons emitted by the target or surroundings that are scattered is a function of the detailed geometry and the cross-sections of the scatterers. Most of the scattering will be from nuclei in the explosives or soil, but the complex geometry precludes a simple analysis. One of the tasks of the nuclear modelling is to determine the significance of the scattering.

Energy straggling in the thick target of the compact gamma-ray generator is an additional potential source of energy broadening, but the 7-keV resonance width of the photon production reaction ensures emitted gamma-rays with a narrow energy profile [9].

Table 1: Discrete photoneutron energies (MeV) from major elements in soil, explosives and air for E_γ = 11.668, 6.128 and 4.439 MeV. Nitrogen energies and possible interferences (within resolution of spectrometer) are bold faced.

Isotope	^{2}H	^{13}C	^{14}N	^{15}N	^{17}O	^{18}O	^{29}Si	^{30}Si	^{56}Fe	^{57}Fe		^{40}Ar
% Natural Abundance	0.015	1.1	99.634	0.366	0.038	0.200	4.670	3.100	91.720	2.200		99.6
Q-value (MeV) [17]	2.225	4.946	10.553	10.833	4.143	8.046	8.474	10.609	11.197	7.646		9.869
E_γ =11.668 MeV												
	4.722	6.205	**1.035**	**0.779**	7.082	3.422	3.084	**1.023**	0.462	3.951	3.119	1.754
		2.107			1.389	2.600	1.367		0.058	1.903	1.340	0.519
					1.312	0.537				**1.061**	**1.043**	0.275
					0.570					0.886	0.883	
					0.384					0.640	0.622	
										0.566	0.563	
										0.413	0.408	
										0.261	0.187	
										0.163		
E_γ =6.128 MeV												
	1.952	1.091			1.868							
E_γ =4.439 MeV												
	1.107				0.278							

3. Proposed Apparatus

3.1. Neutron Spectrometer

To provide the high energy resolution necessary to separate the various discrete neutron energies, the use of a ^{3}He ionization chamber is proposed. A suitable one is the FNS-100 neutron spectrometer manufactured by Bubble Technology Industries, Chalk River, Canada. The world-wide shortage of ^{3}He [18] does not affect present availability, but its long term effect is not known.

Neutron energy resolution, which is roughly linear with energy, is approximately 18 ± 2.5 keV at thermal energy, 25 ± 2 keV at 1 MeV and 40 ± 4.5 keV at 2 MeV. It is estimated to be ~65 keV at 4 MeV and ~94 keV at 6 MeV, although it has not been measured [11]. The intrinsic efficiency is moderate, being 3×10^{-4} at 1-MeV neutron energy. In the energy range of interest, the efficiency is smooth and decreases slowly with increasing neutron energy, from 1.6 at 0.2 MeV to 0.6 at 2.5 MeV [11]. From theoretical considerations [11], it is estimated to be 0.3 at 4 MeV and 0.09 at 6 MeV, although again it has not been measured.

The instrument is not very sensitive to high energy (> 10-keV) gamma rays and neutron/gamma discrimination is not a major problem [11]. Detailed information may be found in Refs. [9, 11].

3.2. Compact Gamma-ray Source

The proposed compact gamma-ray source uses the well known resonance at 163 keV (0.157 mb, 7 keV width) of the ^{11}B(p, γ)^{12}C nuclear reaction to produce monoenergetic gamma rays [19]. The reaction produces a pair of 4.439-MeV and 11.668-MeV gamma rays 97% of the time and a 16.107-MeV gamma ray 3% of the time. The presence of the 4.439-MeV gamma ray does not significantly complicate the neutron spectra due to the 11.668-MeV gamma ray, as will be discussed in Section 5.2. The 16.107-MeV gamma ray, however, does. Although representing only 3.1% of the intensity of the 11.668-MeV gamma ray, the 16.107-MeV gamma ray produces many additional discrete neutron energies which are mostly resolvable. Further, the higher energy leads to production of broad continuous neutron distributions due to reactions with three or more final state particles, such as (γ,nα), (γ,np), (γ,2n). The effect of this will be examined further in Section 5.2.

Prototypes, developed by Lawrence Berkeley National Laboratory and Sandia National Laboratories, have demonstrated that gamma-ray yields of 2.0×10^{5} s^{-1} and 3.0×10^{6} s^{-1} should be easily achievable [20]. Optimistic extrapolations suggest that gamma-ray rates of 6×10^{8} s^{-1} are possible. The angular distribution of the emitted gamma rays is roughly isotropic, with an anisotropy (maximum deviation/maximum value) of 18.7% over all angles, but only 3.5% over the field of view of the target in the present application (Fig. 1) [9].

A prototype tandem tube generator [21] can produce an accelerating potential of 340 kV, allowing it to also use the ^{19}F(p, $\alpha\gamma$)^{16}O reaction (160 mb). The 6.128-MeV gamma-ray rate is expected to be similar to the 11.668-MeV rates for the single-ended tube. Both tubes have been successful prototypes, although there are still some issues to be resolved.

4. Modelling Description

There are a number of potential obstacles to successful implementation of the method. The first is whether the different relevant materials can be discriminated and quantified by measuring the intensity of the spectral peaks corresponding to their characteristic discrete neutron energies. This, in turn, is a function of the energy levels of the residual nuclei, the incident photon energies, the reaction Q-values and the energy-dependent

response of the detector. It also depends on the contribution of continuum neutrons due to reactions with three or more final particles. Finally, energy broadening due to elastic scattering of neutrons can obscure closely separated spectral peaks. Even if discrimination is theoretically possible, estimates of the expected count rates in practical geometries must be obtained to determine if detection can be achieved in a practical time period. The photoneutron background due to materials in the source, detector, shielding and vicinity must be estimated and optimal placement of shielding must be determined. All of these factors depend on the choice of source, detector and shielding geometry.

Even for simple practical scenarios, the geometry is too complex to allow analytical calculations of many of the factors. Of course, the information could be obtained experimentally. While DRDC Suffield owns an FNS-100 neutron spectrometer, the compact gamma-ray source is not yet commercially available. For laboratory purposes, the source could be mimicked by a proton beam from a low energy particle accelerator, such as a Van de Graaff, on a ^{11}B target. Such a facility was not readily available to us, so it was decided to first do simulations to answer some of the questions.

Modelling can provide answers that are difficult to obtain experimentally, such as the exact energy of neutron groups. The relative contributions to the spectrum from different materials and locations can be assessed by tagging trajectories. By turning scattering on and off, its effects on energy broadening can be determined, as well as the contribution to background due to down-scattering of ^{2}H photoneutrons. Unlike in a real gamma-ray generator, different gamma-ray energies can be turned on and off, allowing their contributions to be isolated. Lastly, when optimizing the geometry, many combinations of target, source and detector positions and target and shielding materials can be tried in less time and at less expense than experimentation.

The modelling was conducted using Geant4 [22, 23]. A simulation and data analysis system was created by integrating the ROOT data analysis framework [24] libraries with the Geant4 libraries. By employing objects of the "TTree" class, high level methods could be used to access a variety of particle parameters, such as kinetic energy, flight time, position and momentum, from either the vertex of production, the position of detection or both. Different particles can be chosen for tracking, allowing both photoneutron detection rates and background gamma rates to be evaluated.

4.1. Model Physics and Validation

It was necessary to ensure that the photoneutron production simulation in Geant4 was a useful approximation to reality for our problem. Photoneutron cross-section data in the 6- to 12-MeV range which could be used to populate Geant4 mostly come from neutron capture and broad energy sources. There are very limited data from neutron capture sources (e.g., Refs. [11, 25]) and these consist of only a small number of discrete photon energies of very narrow widths (~ few eV). From a statistical view point, such measurements would be expected to be off-resonance. The bulk of the available data derived from quasi-monoenergetic broad energy sources, such as stepped bremsstrahlung or positron annihilation in flight, which average over the resonances and off-resonance regions and thus would be expected to be larger than those from neutron capture gamma rays.

Table 2: Geant4 and experimental photoneutron cross-sections of light nuclei at or near 11.7 and 16.1 MeV.

Target	E_γ (MeV)	Geant4 (mb)	Experimental (mb)	Geant4/ Experimental
^{14}N	11.7	0.06	0.54 [26]	0.11
^{15}N	11.7	0.29	1.49 [27]	0.19
^{17}O	11.7	0.50	1.26 [28]	0.40
^{18}O	11.7	0.57	6.66 [29]	0.09
^{29}Si	11.7	1.35	3.38 [30]	0.40
^{29}Si	16.1	13.94	5.42 [30]	2.6
^{30}Si	13.4	3.95	7.04 [30]	0.56
^{30}Si	15.6	11.11	13.86 [30]	0.80

Geant4 offers a number of models for photoneutron production that yield somewhat different results depending on the problem being simulated. A direct comparison between the available cross-section data in the literature and the different models revealed that the "Quark Gluon String with Precompound Binary Cascade Model with High Precision Neutron Interactions (QGSP_BIC_HP)" was much more accurate than the other models tested and was thus selected for all subsequent simulations.

To compare cross-sections for Geant4 photoneutron processes with experimental values, a simple geometry was chosen which consisted of a pencil beam, incident on a half space of target material, surrounded by a spherical detector. Low-Z materials expected to be found in this application (Table 1) were examined. Gamma-ray energies were selected at regular intervals in the energy range of interest (Q-value to 16.1 MeV) and histograms of the number of neutrons per incident gamma ray versus neutron kinetic energy were generated and used to calculate the effective cross-sections employed by Geant4. Neutron spectra and cross-sections were compared to published measured broad energy source data. (There are no truly monoenergetic source data for comparison for the light nuclei.) Table 2 compares Geant4 and experimental broad energy source photoneutron cross-sections at or near 11.7 and 16.1 MeV. Several high-Z nuclei near the closed shell in Pb (Ta, Tl, Au, Pb and Bi) were also examined because published measured photoneutron cross-sections from monoenergetic neutron capture gamma rays in the relevant energy range are available [11]. Graphs comparing Geant4 and experimental cross-sections versus gamma-ray energy are found in [9].

The overall behavior of cross-sections for heavy and

light nuclei suggests that Geant4 overestimates the neutron yield compared to truly monoenergetic photon sources, such as from thermal neutron capture. For the light nuclei of interest near 11.7 MeV, Geant4 underestimates broad energy source experimental data by a factor of roughly 3-12. The energy spread of the ^{11}B(p,γ) reaction will be several keV wide at resonance which is roughly an order of magnitude narrower than differential bremsstrahlung energy spreads but three orders of magnitude wider than those of thermal capture beams. Thus measured cross-sections from the reaction should be expected to lie between those measured using broad energy spectra and narrow energy spectrum photons, but much closer to the former since they will be averaged over many resonances. The Geant4 cross-section values generally lie in this range, suggesting that they are reasonable, although possibly somewhat low estimates for this application. Nevertheless, more monoenergetic photoneutron experimental data is needed in the relevant energy range, particularly from the ^{11}B(p,γ) reaction, to incorporate into Geant4.

It was also observed that, for a number of likely reasons [9], only neutrons corresponding to the ground state of product nuclei were generated. To improve model fidelity by allowing photoneutron emission from excited states of the product nucleus, the Geant4 "G4ChiralInvariantPhaseSpace" class was modified. Whenever a hadron is created, that class determines if it is a neutron and then calls two member functions from a new class, "G4PhotoNeutronExcitationDataSet". The latter class contains an array of excited states for a number of the common product nuclei applicable to the present problem. One member function determines if the photoneutron corresponds to a product nucleus in the class array. If true, a second member function selects an excitation level for the product nucleus at random, using the branching ratios as weights, and modifies the energy of the photoneutron accordingly. Presently, branching ratios are calculated by equipartition of the photoneutron cross-section among all energetically favorable excited states of the product nucleus. There is no theoretical justification for equipartition, but experimental photoneutron spectra from heavy nuclei using neutron capture gamma rays near the energy range of interest show that branching ratios to various levels are typically within an order of magnitude of one another [11]. The model modifications should then allow interference between neutron groups to be examined in a qualitative, if not quantitative, fashion. Simulations were run using both the original and the modified Geant4 code. At 11.668-MeV excitation only a few excited states are energetically favorable and including them has a small impact on the spectra. At 16.107 MeV, numerous excited states are accessible. Most can be resolved by the neutron detector but often not in the simulated spectra. (Because of the low number of events per simulation, energy binning was typically 0.070-0.100 MeV). Thus the preliminary results which follow make only limited use of the modified model. Unless stated otherwise, the standard Geant4 model was used for all spectra.

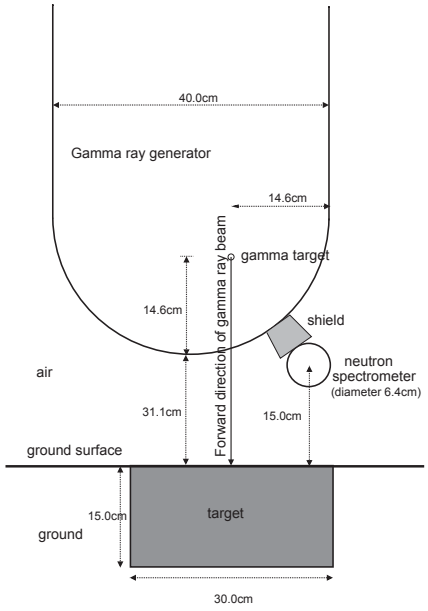

Figure 1: Geometry for photoneutron detection of an explosive device (target) in the ground. The symmetry axis of the cylindrical neutron spectrometer is perpendicular to the page. Proton direction and hence forward direction of gamma-ray emission is vertically downward.

4.2. Buried Bulk Explosives Detection Geometry

Fig. 1 presents a simple geometry for confirmation of an explosive-filled target buried in soil using photoneutron spectroscopy with monoenergetic gamma rays. The target size is typical of an antitank landmine. Dimensions of the photon generator were derived from King *et al.* [20] and are considered approximate. Relative positions of source, detector and target, and shield thickness and position have not been optimized, but rather are illustrative of possible final dimensions. The angular distribution of the gamma rays emitted by the source was obtained from Ref. [20]. This geometry will be used exclusively in the results that follow, with ground, target and shield materials being varied.

5. Modelling Results

5.1. Spectra For 11.668-MeV Gamma Rays

The simulated neutron spectrum at the unshielded detector position due to a landmine target made of RDX ($C_3H_6N_6O_6$) in air irradiated by 11.668-MeV gamma rays is shown in Fig. 2. In this and other spectral plots to follow, the energy dependent efficiency and response function of the neutron detector have not been taken into account. As discussed in Section 3.1, the efficiency is small and has a smooth and slowly varying energy dependence in the range of interest. The implications will be discussed later. The main effects of the response

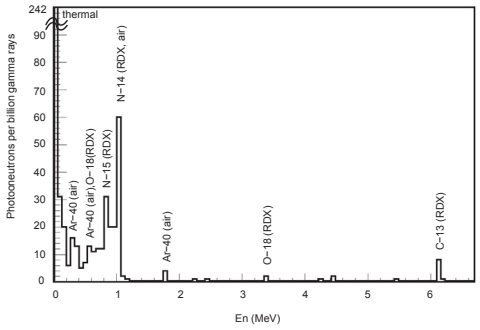

Figure 2: Simulated neutron spectrum at unshielded detector position for RDX landmine target in air irradiated by 11.668-MeV gamma rays. Note break at top of vertical scale. Photoneutron groups are labelled by isotope of origin. Modified model with excited states turned on was used.

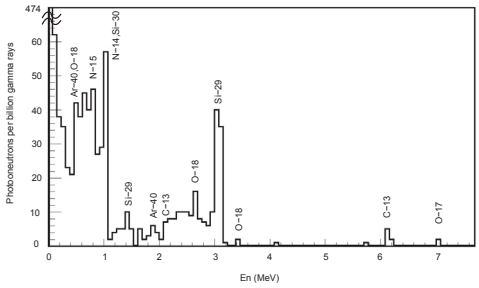

Figure 3: Simulated neutron spectrum at unshielded detector position for RDX landmine target in sand irradiated by 11.668-MeV gamma rays. Note break at top of vertical scale. Photoneutron groups are labelled by isotope of origin. Modified model with excited states turned on was used.

function are broadening of the peaks and the addition of a continuum. However, the broadening is less than the energy bin widths of the plots and the continuum can be removed in spectral processing. The two dominant, well resolved peaks are due to nitrogen from RDX with a small contribution from air. Small peaks are also present due to the ^{13}C and ^{18}O in RDX[2]. The continuum between the nitrogen peaks and below the ^{15}N peak and the large zero energy (thermal) peak are due to neutron scattering in the target. This is verified by the absence of the continuum and thermal peak in the spectrum of neutrons at the point of their initial production. (This so-called production spectrum is not shown.)

The simulated neutron spectrum at the unshielded detector position due to an RDX landmine target in pure sand (SiO_2) irradiated by 11.668-MeV gamma rays is shown in Fig. 3. The separation in energy between the photoneutron peak due to ^{30}Si in sand (~ 1.023 MeV) and that due to the ^{14}N of the explosives (~ 1.035 MeV) is less than the resolution of the neutron spectrometer. Fortunately, the relative contributions of nitrogen and silicon can still be determined by other peaks, notably the ^{29}Si near 3.084 MeV and the ^{15}N peak near 0.779 MeV. The 4.439-MeV gamma rays, which have the same intensity as those at 11.668 MeV, have been excluded from the simulations, since their energy is so low that only ^{17}O and ^{2}H are excited. The former is of insufficient natural abundance to be observed, as evidenced by the absence of any ^{17}O-related neutron groups due to 11.668-MeV gamma rays. The 1.107-MeV neutrons from ^{2}H are near in energy to the 1.023/1.035 MeV ^{14}N/^{30}Si peak, however the expected intensity is very low due to the low natural abundance of deuterium and the small cross-section at 4.439 MeV. Moreover, their separation would be easily resolved by the neutron spectrometer.

[2]Identical simulations with only air present yielded on average nine photoneutrons in the ^{14}N peak, two in the ^{40}Ar peak and none in the ^{15}N and ^{18}O peaks.

5.2. Effect of 16.107-MeV Gamma Ray

The simulated neutron spectrum at the unshielded detector position due to an RDX landmine target in sand is shown in Fig. 4. The target has been irradiated by 11.668 and 16.107-MeV gamma rays in a 97/3 intensity ratio. Even with the substantially smaller intensity of the 16.107-MeV gamma ray, complications to the spectrum are evident, partly due to the general increase in photoneutron cross-sections with increasing gamma-ray energy. Increased numbers of continua are observed as three body photodisintegration reactions, such as ^{14}N(γ,np)^{12}C (E_n^{max}=3.352-MeV neutron endpoint energy) and ^{17}O(γ,nα)^{12}C (E_n^{max}=4.519 MeV), become energetically favorable. One potential advantage of the mixed energy beam is that the ^{14}N and ^{30}Si peaks which were separated by 0.012 MeV at 11.668-MeV excitation energy are separated by 0.157 MeV at 16.107 MeV. (The neutron energy spectra are presented here in ~0.10-MeV bins, so the two neutron groups at 5.157/5.314 MeV appear to be merged on the spectral plots.) Thus, the unresolved peaks at the 11.668-MeV gamma-ray energy would be resolved at 16.107 MeV (Section 3.1), which could allow improved estimation of the nitrogen/silicon ratio.

In any case, the main peaks contributed by the explosive are still visible and well resolved and the presence of nitrogen and carbon can be seen. Including product nuclear excited states in the model slightly complicates the spectrum (Fig. 5). The separation of the relevant peaks is not as obvious as in Fig. 4, due to the coarse energy binning, but they are nevertheless resolved.

5.3. Neutron Scattering and Geometry Effects

The effect of scattering and detector geometry can be evaluated by comparing spectra at the detector position with spectra at the point of initial photoneutron production (not shown). The latter have, as expected, very narrow widths for each reaction energy (essentially single bins) and much higher count rates compared to the former. For example, the count rate for the 1.035/1.023-MeV nitrogen/silicon peak in Fig. 3 is roughly 300 times lower than the corresponding peak in

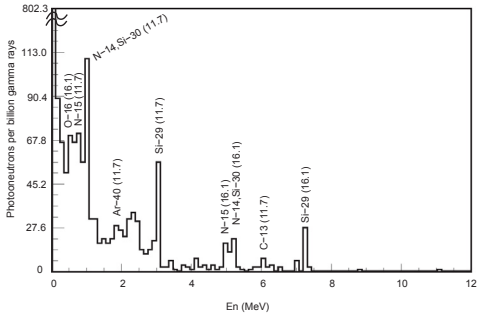

Figure 4: Simulated neutron spectrum at unshielded detector position for RDX landmine in sand irradiated by 11.668 and 16.107-MeV gamma rays in a 97/3 intensity ratio. Note break at top of vertical scale. Photoneutron groups are labelled by isotope of origin and, in brackets, the energy in MeV of the excitation gamma ray.

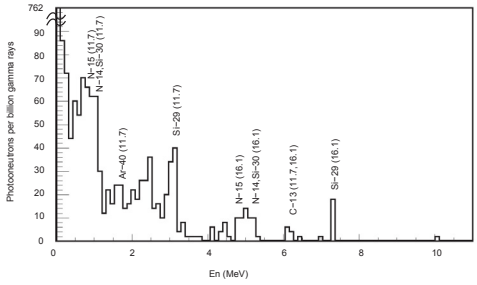

Figure 5: Simulated neutron spectrum at unshielded detector position for RDX landmine in sand irradiated by 11.668 and 16.107-MeV gamma rays in a 97/3 intensity ratio. Note break at top of vertical scale. Photoneutron groups are labelled by isotope of origin and, in brackets, the energy in MeV of the excitation gamma ray. Modified model with excited states turned on was used.

the production spectrum. This significant reduction is due in part to geometrical factors, but also to the effects of neutron scattering between the site of production and the detector. This is evident in the spectral continuum below 1 MeV and 3 MeV in Fig. 3 but is completely absent in the production spectrum. There is only one reaction at this excitation energy that can produce a continuous neutron spectrum, ^{17}O(γ,nα)^{12}C, E_n^{max}=0.341 MeV. However, the natural abundance of ^{17}O is so low that it would not contribute more than one or two neutrons to the spectrum. (This is confirmed by its absence in the production spectrum.) Further evidence of the significant neutron scattering due to sand can be seen by comparing the spectrum at the detector position for RDX in sand (Fig. 3) with the corresponding spectrum for RDX in air (Fig. 2). Fortunately, inspection of Fig. 3 reveals that neutron scattering does not significantly impede the ability to separate the relevant photoneutron peaks in this application.

5.4. Detection of Homemade Explosives

Some homemade explosives contain no nitrogen and so cannot be readily detected using some common nuclear explosives confirmation techniques, such as thermal neutron activation [31]. They are detectable in some scenarios by fast neutron activation. However, when buried in soil, interference peaks from silicon and oxygen obscure the carbon and nitrogen peaks and so the more complicated associated particle method must be employed [32]. To see if the photoneutron spectroscopy method might be useful for detection of such nonconventional explosives, a simulation was done using a target of triacetone triperoxide (TATP: $C_9H_{18}O_6$). At a glance it would seem that using 6.128-MeV gamma rays would be the best approach because they would excite so few background materials (Table 1). However, the low photoneutron cross-sections at that energy and the low isotopic abundances conspire to produce only a few ^{13}C photoneutrons in the TATP per billion source gamma rays, and yield on average zero at the detector position.

By comparison, the simulated neutron spectrum at the unshielded detector position for the same TATP target in air irradiated by 11.668 and 16.107-MeV gamma rays in a 97/3 intensity ratio is shown in Fig. 6. The number of ^{13}C neutrons is nonzero, but small. The peak near 6 MeV is well isolated and would remain so even if sand were present (Fig. 4). Nevertheless, neutron rates from TATP at the detector position are exceedingly low for 6.128-MeV gamma rays and are very low for 11.668 and 16.107-MeV gamma rays.

5.5. Effect of Shielding

So far it has been assumed that no shielding was used. Although the ^{3}He ionization chamber is insensitive to gamma rays, as discussed earlier, very high incident gamma-ray rates might yield a measurable response in

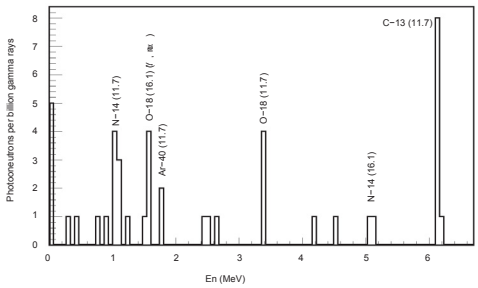

Figure 6: Simulated neutron spectrum at unshielded detector position for a landmine-sized TATP target in air irradiated by 11.668 and 16.107-MeV gamma rays in a 97/3 intensity ratio. Photoneutron groups are labelled by isotope of origin and, in brackets, the energy in MeV of the excitation gamma ray.

Table 3: Shielding material properties for photoneutron spectroscopy near 11.7 MeV. All have a natural isotopic abundance of 100% except for $_{20}Ca^{40}$ which has an abundance of 96.941%.

Element	Q-value (MeV)	Cost ($/100g)	ρ (g/cm^3)	μ/μ_{Pb}
$_{13}Al^{27}$	13.057	0.12	2.7	0.046
$_{15}P^{31}$	12.311	4	1.8	0.036
$_{39}Y^{89}$	11.476	220	4.5	0.21
$_{21}Sc^{45}$	11.324	1400	3.0	0.080
$_{20}Ca^{40}$	15.643	0.44	1.55	0.17

the low energy region of the neutron spectrum which could potentially interfere with the analysis of low energy neutron groups. Thus some gamma-ray shielding may be desirable between the gamma-ray source point and the detector sensitive volume. In order to limit the scope of the study, optimization of the size, shape and position of the shield was not attempted. Instead, an initial study was done to determine the most suitable shielding material for a shield positioned as in Fig. 1. TATP was selected as the target material, since as seen earlier, it yields challengingly few photoneutrons per source gamma ray.

Unfortunately, most high-Z materials have photoneutron Q-values well below 11.7 MeV. A search was made of materials with photoneutron Q-values above or no more than a few hundred keV below 11.7 MeV. (All practical shield materials have photoneutron Q-values less than 16.1 MeV.) The valid candidates were then evaluated, considering gamma-ray shielding effectiveness with respect to Pb (μ/μ_{Pb}, μ being the linear attenuation coefficient), relevant material properties, availability and cost. Properties of the top five candidates are shown in Table 3. Ca^{40} is comparable in gamma-ray shielding performance to the best candidates and produces no neutron background. However, 3.059% of the natural abundance of calcium is composed of five other isotopes, all of which have Q-values below 11.7 MeV.

Fig. 7 presents a simulated neutron spectrum at the detector position for a landmine-sized TATP target in air irradiated by 11.668 and 16.107-MeV gamma rays in a 97/3 intensity ratio. A natural calcium shield is situated between the gamma-ray source and the neutron detector. In spite of the additional calcium isotopes, the background spectrum is significantly lower than that of the second best performer, an aluminum shield (spectrum not shown). Aluminum and yttrium both produce high energy photoneutrons (~3 and 4.5 MeV) that are down-scattered to yield broad continua extending to zero energy which can interfere with target photoneutrons of interest in this application. The primary photoneutron peak from calcium is at ~0.6 MeV, so down-scattering is not of much concern. A much smaller secondary peak near 4.9 MeV has too low a yield to produce noticeable down-scattering. Interference with target photoneutrons of interest is small. Furthermore, the shield photoneutrons can be treated as a constant background to be subtracted, but they will still contribute to increased statistical uncertainty in estimating the peak areas of the neutrons of interest.

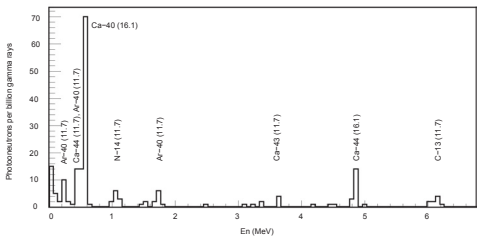

Figure 7: Simulated neutron spectrum at detector position for a landmine-sized TATP target in air irradiated by 11.668 and 16.107-MeV gamma rays in a 97/3 intensity ratio. A natural calcium shield is situated between the gamma-ray source and the neutron detector. Photoneutron groups are labelled by isotope of origin and, in brackets, the energy in MeV of the excitation gamma ray.

Because of the exponentially decreasing gamma-ray response with energy and the 0.764-MeV offset for thermal neutrons, it is not necessary to decrease the gamma-ray rate at the position of the neutron spectrometer to background levels. Since the shielding effectiveness of natural calcium is substantially inferior to that of Pb, any benefit that may be gained by the small reduction in background gamma-ray rates (Section 3.1) may not be worth the penalty due to increased neutron interference. Thus, a thicker shield would likely not be advantageous and it may be best to have no shield at all. Another alternative is to use a type of graded shielding. If sufficiently thin, a layer of high-Z material coupled with a thicker layer of low-Z material may provide sufficient gamma-ray reduction without significant photoneutron production. This should be examined further.

5.6. Photoneutron Rates and Detection Times

In order to be operationally useful, confirmation of bulk explosives requires detection times of a few minutes or less. If we take as an example the 1.035-MeV neutron peak from ^{14}N excitation by 11.668-MeV gamma rays, the count rate in the peak is ~ 60 neutrons per 10^9 source gamma rays. If the photon source is assumed to have a high but achievable rate of 10^8 gamma rays/second, 6 neutrons/second intersect the detector

volume. However, the neutron detector intrinsic efficiency of 3×10^{-4} at 1 MeV means that the detection rate is $\sim 2 \times 10^{-3}$ counts per second. This is not practical with the presently envisioned equipment and geometry. The 6.205-MeV ^{13}C peak results in a detection rate which is two orders of magnitude smaller and hence is even less practical. The detection rate of ^{13}C using 6.128-MeV photons is weaker still.

Although the estimated detection rate is not promising, there are a number of factors that might improve it. The positions of source, detector and target were not optimized for detection rate in this study. Since the number of ^{14}N neutrons produced at the target is more than two orders of magnitude higher than the number that reaches the neutron spectrometer, optimization of the geometry could significantly increase the neutron rate at the detector. The previous count rate estimate included only the ^{14}N photoneutrons from 11.668-MeV gamma rays. If we include all photoneutron peaks from both nitrogen isotopes for 11.668 and 16.107-MeV gamma rays, the yield will increase by about 5%. Further, the previous spectra show that the photoneutron peak height due to ^{29}Si in the sand is roughly 1/2 of that due to ^{14}N. The silicon peaks can be used as a void detector and if they are included, the effective differential rate (difference in rate with and without explosives present) can increase by as much as 50%. By relaxing the constraints on generator size, it may be possible to build higher rate gamma-ray sources. Improved detector efficiency or increased number of detectors may significantly increase the detection rate. Other scenarios for detection of hidden explosives may have higher detection rates due to improved geometry and a reduction of neutron scattering and absorption by an intervening medium. Also, as mentioned in Section 4.1, the simulation code may have somewhat underestimated the photoneutron cross-sections. Thus detection times for TNA and photoneutron spectroscopy of bulk explosives might be expected to be comparable.

6. Conclusions

A new method for detection of bulk explosives based on photoneutron spectroscopy with monoenergetic photons has been presented. Suitable neutron spectrometers were identified that are commercially available and suitable gamma-ray sources exist as prototypes. Analysis and Geant4 simulations have shown that the resulting neutron spectra may be used to identify isotopes associated with explosives. Simulations have shown that discrete neutron energies are sufficiently separated, and neutron elastic scattering effects small enough, that spectral interference from different materials does not impede identification. Induced neutron backgrounds from shielding materials can be problematic, but are not insurmountable. Detection rates for the modelled geometry are at the extreme lower limit of practicality. However, a number of factors may improve the count rate so that detection of explosives buried in soil or hidden in other scenarios may be feasible.

Refinement of the modelling code is necessary. More monoenergetic photoneutron experimental cross-section data is needed in the 6- to 16-MeV range, particularly from the ^{11}B(p,γ) reaction but also from thermal neutron capture sources. The data should be incorporated into the existing Geant4 code, together with inclusion of non-ground state neutrons in a more refined way than the ad hoc approach used here.

To better quantify expected capability, further modelling and experimental studies are needed. The geometry has not been optimized, unforeseen effects due to photoneutron emission from ^{2}H irradiated by 4.439-MeV gamma rays must be evaluated, shielding must be optimized, and modelling must be further validated by experiment. Sand-box experiments can use a Van de Graaff accelerator to simulate the final compact monoenergetic gamma-ray source and geometries and shielding suggested by modelling studies.

References

[1] W. Coleman, R. Ginaven, G. Reynolds, Nuclear methods for mine detection - Volume III Encyclopedia, AD AD919475, U.S. Army Mobility Equipment Research and Development Center, Ft. Belvoir, Virginia (May 1974).

[2] R. Moler, Workshop report: Nuclear techniques for mine detection research, AD A167 968, Belvoir Research and Development Center, Ft. Belvoir, Virginia (July 1985).

[3] L. Grodzins, Nuclear techniques for finding chemical explosives in airport luggage, Nuclear Instruments and Methods in Physics Research Section B 56/57 (1991) 829–833.

[4] A. Buffler, Contraband detection with fast neutrons, Radiation Physics and Chemistry 71 (2004) 853–861.

[5] R. C. Runkle, T. A. White, E. A. Miller, J. A. Caggiano, B. A. Collins, Photon and neutron interrogation techniques for chemical explosives in air cargo: a critical review, Nuclear Instruments and Methods in Physics Research Section A 603 (2009) 510–528.

[6] J. E. McFee, H. R. Andrews, E. T. H. Clifford, A. A. Faust, H. Ing, T. Cousins, D. Haslip, The feasibility of neutron moderation imaging for land mine detection, International Journal of Subsurface Sensing Technologies and Applications 4 (3) (2003) 209–240.

[7] L. E. Beghian, S. Wilensky, A fast neutron spectrometer capable of nanosecond time gating, Nuclear Instruments and Methods in Physics Research Section 35 (1) (1965) 34–44. doi:10.1016/0029-554X(65)90004-2.

[8] A. Zimbal, M. Reginatto, H. Schuhmacher, L. Bertalot, B. Esposito, F. Poli, J. M. Adams, S. Popovichev, V. Kiptily, A. Murari, Compact NE213 neutron spectrometer with high energy resolution for fusion applications, Review of Scientific Instruments 75 (10) (2004) 3553–3555. doi:10.1063/1.1787935.

[9] J. E. McFee, A. A. Faust, K. A. Pastor, Feasibility of bulk explosives detection using photoneutron spectroscopy, in: R. S. Harmon, J. H. Holloway, J. T. Broach (Eds.), Detection and Sensing of Mines, Explosive Objects and Obscured Targets XV, Vol. 7664, 2010, p. 76641I. doi:10.1117/12.849533.

[10] J. M. Cuttler, S. Shalov, Y. Dagan, A high-resolution fast-neutron spectrometer, Transactions of the American Nuclear Society 12 (1) (1969) 63.

[11] J. E. McFee, Photoneutron Spectroscopy of the Nuclei Near Mass 200, Ph.D. thesis, Department of Physics, McMaster University, Hamilton, Canada (1977).

[12] Y. Wang, M. Nastasi, Handbook of Modern Ion Beam Materials Analysis Second Edition, Materials Research Society, Warrendale, Pennsylvania, 2009.

[13] J. E. McFee, Y. Das, Review of unexploded ordnance detection methods (U), Report 292, Defence Research Establishment Suffield, Ralston, AB, Canada (September 1981).

[14] J. E. McFee, A. F. M. Ishaq, T. J. Kennett, W. V. Prestwich, Study of the ^{209}Bi(γ, n)^{208}Bi reaction at 9 MeV, Physical Letters 55B (1975) 369–372.

[15] J. E. McFee, W. V. Prestwich, T. J. Kennett, The photoneutron spectrum of lead following excitation by 8999, 8533 and 8120 keV photons, Physical Review C13 (1976) 1864–1873.

[16] R. B. Firestone, V. S. Shirley, C. M. Baglin, S. Y. F. Chu, J. Zipkin (Eds.), Table of Isotopes Eighth Edition, John Wiley and Sons, New York, 1996.

[17] National Nuclear Data Center, Q-value Calculator (QCalc), http://www.nndc.bnl.gov/qcalc, last accessioned 03 July 2012.

[18] R. T. Kouzes, J. H. Ely, L. E. Erikson, W. J. Kernan, A. T. Lintereur, E. R. Siciliano, D. L. Stephens Jr, D. C. Stromswold, R. M. Van Ginhoven, M. L. Woodring, Neutron detection alternatives to 3he for national security applications, Nuclear Instruments and Methods in Physics Research Section A 623 (3) (2010) 1035–1045. doi:10.1016/j.nima.2010.08.021.

[19] J. Reijonen, N. Andresen, F. Gicquel, R. Gough, M. King, T. Kalvas, K. N. Leung, T. P. Lou, H. Vainionpaa, A. Antolak, D. Morse, B. Doyle, G. Miller, M. A. Piestrup, Development of advanced neutron/gamma generators for imaging and active interrogation applications, in: T. T. Saito, D. Lehrfeld, M. J. DeWeert (Eds.), Optics and Photonics in Global Homeland Security III, Vol. 6540, 2007, p. 65401P.

[20] M. J. King, A. J. Antolak, K. N. Leung, D. H. Morse, T. N. Raber, B. L. Doyle, Performance of a compact gamma tube interrogation source, in: F. D. McDaniel, B. L. Doyle (Eds.), Application of Accelerators in Research and Industry: 20th International Conference, American Institute of Physics, Fort Worth TX, USA, 2009, pp. 619–623.

[21] A. Persaud, J. W. Kwan, M. Leitner, K. N. Leung, B. Ludewigt, N. Tanaka, W. Waldron, S. Wilde, A. J. Antolak, D. H. Morse, T. Raber, A tandem-based compact dual-energy gamma generator, Review of Scientific Instruments 81 (2010) 02B904–1–02B904–4. doi:10.1063/1.3258028.

[22] S. Agostinelli, J. Allison, K. Amako, et al, G4 - a simulation toolkit, Nuclear Instruments and Methods in Physics Research Section A 506 (3) (2003) 250–303.

[23] J. Allison, K. Amako, J. Apostolakis, et al, Geant4 developments and applications, IEEE Transactions on Nuclear Science 53 (1) (2006) 270–278.

[24] R. Brun, F. Rademakers, ROOT - an object oriented data analysis framework, Nuclear Instruments and Methods in Physics Research Section A 389 (1997) 81–86.

[25] Y. Birenbaum, Z. Berant, S. Kahane, R. Moreh, A. Wolf, E1-E2 interference in ^{159}Tb(γ,n) and ^{209}Bi(γ,n) reactions, Physical Review C 34 (6) (1986) 2055–2064.

[26] B. L. Berman, S. C. Fultz, J. T. Caldwell, M. A. Kelly, S. S. Dietrich, Photoneutron cross sections for Ba^{138} and N^{14}, Physical Review C 2 (6) (1970) 2318–2323. doi:10.1103/PhysRevC.2.2318.

[27] A. D. Bates, R. P. Rassool, E. A. Milne, M. N. Thompson, K. G. McNeill, N^{15} photoneutron cross section, Physical Review C 40 (2) (1989) 506–514. doi:10.1103/PhysRevC.40.506.

[28] J. W. Jury, B. L. Berman, D. D. Faul, P. Meyer, J. G. Woodworth, Photoneutron cross sections for O^{17}, Physical Review C 21 (2) (1980) 503–511. doi:10.1103/PhysRevC.21.503.

[29] J. G. Woodworth, K. G. McNeill, J. W. Jury, R. A. Alvarez, B. L. Berman, D. D. Faul, P. Meyer, Photonuclear cross sections for O^{18}, Physical Review C 19 (5) (1979) 1667–1683. doi:10.1103/PhysRevC.19.1667.

[30] R. E. Pywell, B. L. Berman, J. W. Jury, J. G. Woodworth, K. G. McNeill, M. N. Thompson, Photoneutron cross sections for the silicon isotopes, Physical Review C 27 (3) (1983) 960–975. doi:10.1103/PhysRevC.27.960.

[31] E. T. H. Clifford, J. E. McFee, H. Ing, H. R. Andrews, D. Tennant, E. Harper, A. A. Faust, A militarily fielded thermal neutron activation sensor for landmine detection, Nuclear Instruments and Methods in Physics Research Section A 579 (2007) 418–425. doi:10.1016/j.nima.2007.04.091.

[32] A. A. Faust, J. E. McFee, C. L. Bowman, C. Mosquera, H. R. Andrews, V. D. Kovaltchouk, H. Ing, Feasibility of fast neutron analysis for the detection of explosives buried in soil, Nuclear Instruments and Methods in Physics Research Section A 659 (2011) 591–601. doi:10.1016/j.nima.2011.07.036.